Journal of Sea Research 95 (2015) 45–55

Contents lists available at ScienceDirect

Journal of Sea Research

journal homepage: www.elsevier.com/locate/seares

Seasonal phytoplankton response to physical processes in the southern Yellow Sea

Xin Liu [a], Bangqin Huang [a,*], Qiu Huang [a], Lei Wang [a,e], Xiaobo Ni [b], Qisheng Tang [c], Song Sun [d], Hao Wei [e], Sumei Liu [f], Chaolun Li [d], Jun Sun [e]

[a] State Key Laboratory of Marine Environmental Science, Fujian Provincial Key Laboratory of Coastal Ecology and Environmental Studies, Xiamen University, 361005 Xiamen, China
[b] State Key Laboratory of Satellite Ocean Environment Dynamics, Second Institute of Oceanography, State Oceanic Administration, 310012 Hangzhou, China
[c] Yellow Sea Fisheries Research Institute, Chinese Academy of Fishery Sciences, 266071 Qingdao, China
[d] Key Laboratory of Marine Ecology and Environmental Sciences, Institute of Oceanology, Chinese Academy of Sciences, 266071 Qingdao, China
[e] College of Marine Science and Engineering, Tianjin University of Science and Technology, 300222 Tianjin, China
[f] Key Laboratory of Marine Chemistry Theory and Technology, Ministry of Education, Ocean University of China, 266100 Qingdao, China

ARTICLE INFO

Article history:
Received 22 July 2013
Received in revised form 13 October 2014
Accepted 24 October 2014
Available online 31 October 2014

Keywords:
Seasonal variations
Phytoplankton
Nutrients
Water masses
Ecosystems
Yellow Sea

ABSTRACT

The Yellow Sea (YS) is a semi-enclosed marginal sea in the West Pacific. As part of the China GLOBEC-IMBER program, the present study set out to investigate the mechanisms involved in the seasonal patterns of phytoplankton biomass and community structure in the southern YS. During four cruises in April and October 2006, and March and August 2007, the phytoplankton spring bloom, the Yellow Sea Warm Current (YSWC) and the Yellow Sea Cold Water Mass (YSCWM) were the most remarkable biogeochemical events in the study area, involving significantly different phytoplankton communities. During cold seasons nutrient-rich water was observed, coincident with the occurrence of the YSWC, which is considered to be warm and saline water from the northward Kuroshio branch current (Cheju Warm Current). However, low Chl *a* concentrations (<0.6 mg m^{-3}) and a high relative abundance of prasinophytes (29% of Chl *a*, average value of the euphotic zone, and the same below) were observed in the YSWC area in March. During April a spring bloom occurred with very high concentrations of Chl *a* (7.69 mg m^{-3}) and fucoxanthin (1.98 mg m^{-3}), and was dominated by diatoms. The mechanism and processes of the spring bloom in the central YS are very complex and possibly unique, and the YSWC affects the distribution of nutrients and hydrological environment for phytoplankton growth. Low Chl *a* biomass (0.2 mg m^{-3}) and a low contribution of diatoms, but a high contribution of cyanobacteria (36%) were observed in the stratified central YS in August when the YSCWM prevailed, and a high relative abundance of chrysophytes (38%) was observed in October when the YSCWM was decaying. In a word, significant seasonal variations of phytoplankton biomass and community structure were observed in the central rather than the coastal area. These results were considered as the physical–chemical–biological characteristics of the unique ecosystem in the central YS.

1. Introduction

The Yellow Sea (YS) is a semi-enclosed marginal sea with depths ranging from 20 to 90 m in the western Pacific Ocean, bounded by China and Korea. It is famous for its high productivity and abundant fishery resources. Recently, environmental problems in the YS became the center of interest of oceanographers both in China and Korea and much related research work (e.g. the China GLOBEC-IMBER program and China Jellyfish Program) is in progress (Sun et al., 2011; Tang et al., 2007, 2010).

In the past few decades, a number of studies have been carried out in the YS both to investigate the circulation features and for water mass analysis (Huang et al., 2005; Lie, 1986; Lie et al., 2009; Park, 1986). Based on these studies, four major water masses are often distinguished in the YS. Among them, the Yellow Sea Cold Water Mass (YSCWM) is the most particular phenomenon, and this prevails from summer to fall with the boundary and temperature–salinity structure remaining almost unchanged each year (Zhang et al., 2008; and references therein). Briefly, it occurs in the central YS, and the primary characteristics are strong stratification and a very low temperature (<10 °C) in the deep waters in summer. In winter, the temperature and salinity are higher in the central area than in the surrounding water, which is associated with the Yellow Sea Warm Current (YSWC). As early as 1934, the YSWC was reported as a mean flow transporting saline water originating from the Kuroshio, and oceanic materials from the East China Sea, through the YS (Lie, 1986; Uda, 1934). On the other hand, along both the Chinese and Korean coasts, there are several coastal water currents, which flow southward, especially during winter. These coastal currents

* Corresponding author at: College of the Environment and Ecology, Xiamen University, Xiamen, Fujian 361005, China. Tel./fax: +86 592 2187783.
E-mail address: bqhuang@xmu.edu.cn (B. Huang).

http://dx.doi.org/10.1016/j.seares.2014.10.017
1385-1101/

are usually characterized by low temperature, low salinity and rich nutrients (Chen, 2009). Besides these, the Changjiang (Yangtze) River, as one of the largest rivers in the world, affects both the northern East China Sea and the southern YS. Overall, these water masses interact differently during different seasons (Lie, 1986; Lie et al., 2009).

Although many studies provide strong evidence concerning the circulation features and water mass properties, extensive studies on the biogeochemical responses of these water masses are still needed. It is known that the YSWC transports warm and saline water to the YS, however the nutrient properties and phytoplankton responses of the YSWC are still unclear. The YSCWM not only influences temperature, but also distribution of the phytoplankton biomass, bacterial abundance and production (Hyun and Kim, 2003; Fu et al., 2009; Zhang et al., 2009). Studies show that there are large spatial and temporal variations of size-fractioned Chl *a* in the YS, and picophytoplankton is consistently of absolute dominance (>40%) in the central YS when the YSCWM prevails (Fu et al., 2009; Zhang et al., 2009). On the other hand, this deep cold water mass is a key player in the spatial variations of the dominant zooplankter, *Calanus sinicus* (Wang et al., 2009). Moreover, long-term observations indicate that the YS ecosystem is sensitive to environmental changes, including climate changes and anthropogenic impacts (He et al., 2013; Lin et al., 2005). Although the need for more field work on the ecosystem, particularly the structure and function of the communities and the relationships with biogeochemical processes have been suggested (He et al., 2013; Lin et al., 2005), there have never been any reports concerning the seasonal variations on phytoplankton community composition coupled with the physical processes in the YS.

In previous studies, the YSWC and the YSCWM are observed in the central area in different seasons, thus if the seasonal patterns of phytoplankton biomass and community structure in the central area are different from those in the coastal area. What are the roles of the YSWC and the YSCWM on the distributions of phytoplankton biomass and community structure in the YS? Our goal was to better understand the seasonal phytoplankton response to physical processes in the central YS.

2. Materials and methods

Four cruises were carried out on the R/V Beidou during 14–28 April 2006, 17 October–3 November 2006, 17–23 March 2007 and 3–9 August 2007 (Fig. 1). At each station, hydrographic measurements and water samples were conducted using a Seabird SBE 19 CTD profiler equipped with a 12 Niskin bottle Rosette sampler. Two stations (B2, B3) were not sampled during the April cruise, one station (H2) during the October cruise, and Transect Y (Stations Y2–8) during the August cruise.

Water samples for nutrients and pigments were taken with Niskin water samplers from 3–6 layers in the water column of bottom depth ranging from 30 to 80 m. Nutrient samples were filtered immediately through acid-cleaned 0.45 μm pore size acetate cellulose filters, and the filtrates were poisoned with saturated $HgCl_2$ solution. Nutrients including NO_3^-, NO_2^-, $PO_4^{3-}$and $Si(OH)_4$ were determined using an autoanalyzer (Model: Skalar SAN^{plus}). The precision of nutrient analysis in this study was ≤3%, and the detection limits of NO_3^-, NO_2^-, PO_4^{3-}, and

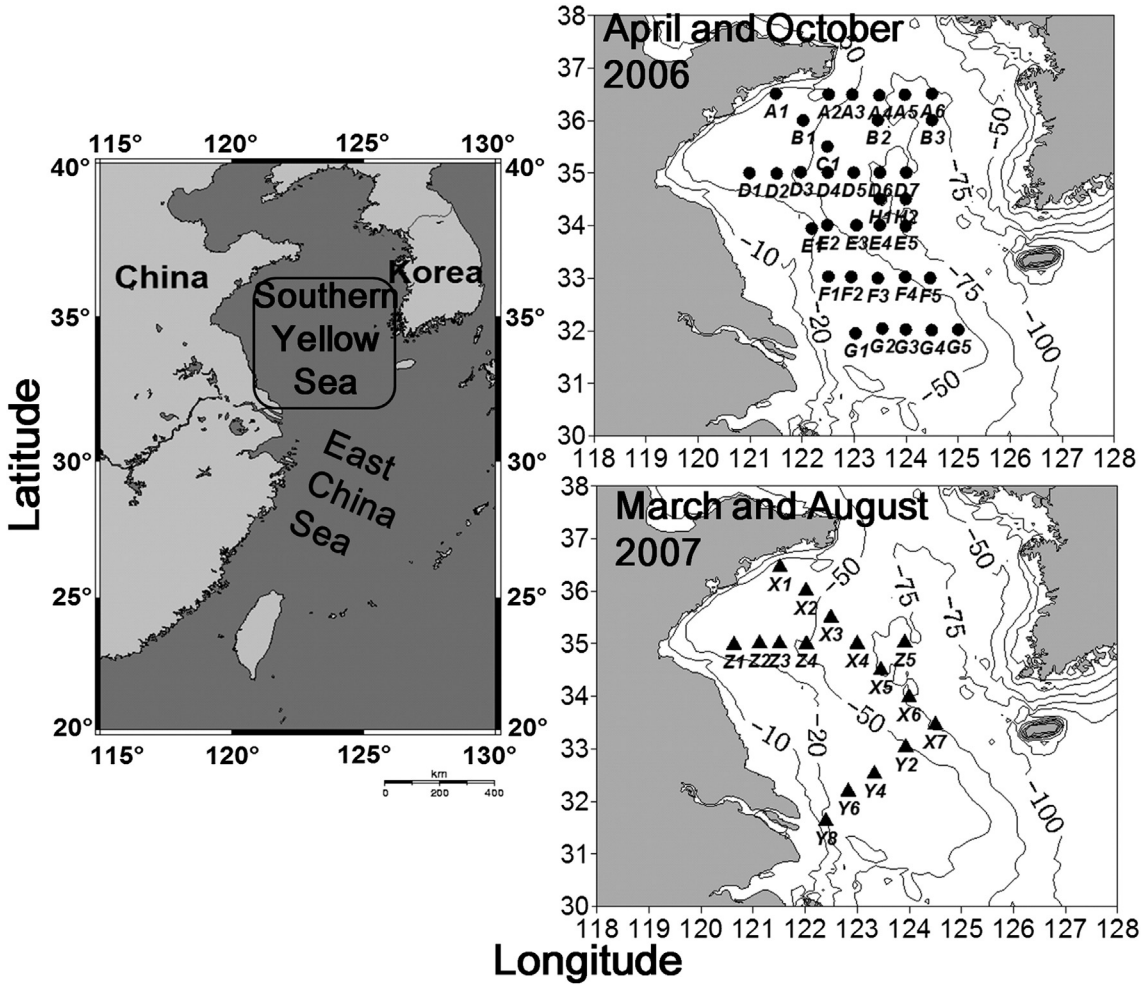

Fig. 1. Map of study area and sampling stations in the southern Yellow Sea during the four cruises in 2006–2007, with isobaths of 10, 20, 50, 75 and 100 m.

$Si(OH)_4$ were 0.014, 0.14, 0.07, and 0.07 μmol L^{-1}, respectively (Liu et al., 2005).

In this study, we used HPLC based measurement of the relative abundance of different phytoplankton groups (Mackey et al., 1996) associated with microscopic observations (Utermöhl, 1958) to confirm the calculated results, especially the dominated group and species. Seawater samples for phytoplankton pigment analysis (4–10 L, based on biomass) were filtered through 47 mm GF/F glass fiber filters (under a vacuum pressure less than 75 mm Hg and in dim light). Pigment samples stored in liquid nitrogen during the cruise, and transferred to a deep freezer (−80 °C) in the laboratory. Generally, the pigment sample analysis was completed within one month after the cruise, and the longest time a sample was stored in the freezer was about 45 days. Phytoplankton pigments were extracted in N, N-dimethylformamide and analyzed using an Agilent series 1100 HPLC system fitted with a 3.5 μm Eclipse XDB C8 column (4.6 × 150 mm, Agilent Technologies, Waldbronn, Germany) (Zapata et al., 2000), using a modification of the method of Mantoura and Llewellyn (1983), Van Heukelem and Thomas (2001) and Huang et al. (2010). Quantification was performed with standards which were purchased from DHI Water & Environment, Hørsholm, Denmark. The following pigments were detected and quantified: chlorophyll *a* (Chl *a*), chlorophyll *b* (Chl *b*), chlorophyll *c*1 + *c*2, chlorophyll *c*3, fucoxanthin, 19′-hexanoyloxfucoxanthin, 19′-butanoyloxfucoxanthin, prasinoxanthin, lutein, zeaxanthin, diadinoxanthin, alloxanthin, neoxanthin, violaxanthin and peridinin. Although the divinyl (DV) Chl *a* standard peak could be separated from the Chl *a* standard peak using the C8 column, DV Chl *a* and DV Chl *b* were not detected in any of the samples.

Based on pigment data, the CHEMTAX (Mackey et al., 1996) program was used to retrieve the group composition of the phytoplankton. CHEMTAX software runs in MATLAB, together with a matrix of field pigment data and the initial input of a matrix of pigment: Chl *a* ratios for each phytoplankton group. The input pigment ratios matrix used in the CHEMTAX calculation was based on knowledge of the common phytoplankton groups present in the YS and adjacent areas (Furuya et al., 2003; Liu et al., 2012). In addition, since pigment ratios change with the light regime, the database was kept separate for different depths as suggested by Mackey et al. (1996). Besides, 10 successive CHEMTAX runs were performed using the output pigment: Chl *a* ratio matrix of each run as input for the following run in order to have these ratios stabilized toward their most probable values (Latasa, 2007). Table 1 lists the initial input pigment: Chl *a* ratio for each group used in this calculation and an example of the final ratio after 10 successive CHEMTAX runs. Initial water samples (250 ml) for microscopic observations were preserved in 1% Lugol's solution until identification. These samples were stored at room temperature in the dark until they were counted using the Utermöhl method (Utermöhl, 1958).

The monthly mean sea surface temperature (SST), Chl *a* and daily sea surface wind (SSW) speed at Stations D1 (coastal) and D5 (central) were extracted from AVHRR, SeaWiFS and QuikSCAT products (Ocean Watch North Pacific Demonstration Project, 2008) from Oct. 1981 to Nov. 2008, Sep. 1997 to Dec. 2009 and Aug. 1999 to Oct. 2009. The resolutions of these three parameters were 0.044, 0.1 and 0.25°.

The 35°N transect passes through the Yellow Sea basin (Fig. 1), where spring bloom, YSWC and YSCWM occurred. It has been designed as a typical transect for observation in the southern Yellow Sea (Liu et al., 2009, 2012). Therefore, we selected this transect to compare the differences of water column structure among these cruises (Fig. 3). For comparison between the central area and the surrounding water masses, the central area and coastal area were defined as the areas with a water depth >50 m and ≤50 m (Fig. 1). A one-way ANOVA was used for statistical analysis following a test for the homogeneity of the variances. The significance level was set at $p < 0.05$. ANOVA results were compared using the least significant difference method, and the phytoplankton biomass (in terms of Chl *a* concentrations) was log-transformed because of the possibly very high variance induced by the patchy distribution of Chl *a*. The mean nutrient and Chl *a* concentrations were calculated as the integrated mean in the euphotic zone (integrated value/depth). The euphotic zone was defined as the upper water column down to the depth at which the downward photosynthetically active radiation (PAR) was 1% of the value just below the surface. Vertical profiles of light intensity (PAR) were obtained at each station using a free-fall spectroradiometer (SPMR, Satlantic), just prior to water sampling.

3. Results

3.1. Physical and chemical characteristics

Based on the horizontal and vertical distribution of temperature, the hydrographic features of the study area could be generally divided into the warm (stratification, August and October) and cold (well-mixing, March and April) seasons (Figs. 2 and 3).

Table 1
Initial input pigment: Chl *a* ratios for all clusters in CHEMTAX analysis (a) and final pigment: Chl *a* ratios of the 10–30 m samples during the October cruise after 10 successive CHEMTAX runs (b).

	Peri	But-fuco	Fuco	Hex-fuco	Neo	Pras	Viola	Allo	Lut	Zea	Chl *b*	Chl *a*
a												
Dinoflagellates	1.06	0	0	0	0	0	0	0	0	0	0	1
Diatoms	0	0	0.47	0	0	0	0	0	0	0	0	1
Chrysophytes	0	0.37	0.11	0	0	0	0	0	0	0	0	1
Prymnesiophytes	0	0	0	1.71	0	0	0	0	0	0	0	1
Chlorophytes	0	0	0	0	0.08	0	0.06	0	0.14	0.01	0.46	1
Cryptophytes	0	0	0	0	0	0	0	0.23	0	0	0	1
Prasinophytes	0	0	0	0	0.1	0.35	0.11	0	0.02	0	0.8	1
Cyanobacteria	0	0	0	0	0	0	0	0	0	0.35	0	1
b												
Dinoflagellates	1.06	0	0	0	0	0	0	0	0	0	0	1
Diatoms	0	0	0.17	0	0	0	0	0	0	0	0	1
Chrysophytes	0	0.37	0.11	0	0	0	0	0	0	0	0	1
Prymnesiophytes	0	0	0	1.71	0	0	0	0	0	0	0	1
Chlorophytes	0	0	0	0	0.04	0	0.03	0	0.07	0	0.16	1
Cryptophytes	0	0	0	0	0	0	0	0.23	0	0	0	1
Prasinophytes	0	0	0	0	0.19	0.43	0.18	0	0.03	0	1.39	1
Cyanobacteria	0	0	0	0	0	0	0	0	0	0.35	0	1

Peri: peridinin; But-fuco: 19′-butanoyloxfucoxanthin; Fuco: fucoxanthin; Hex-fuco: 19′- hexanoyloxfucoxanthin; Neo: neoxanthin; Pras: prasinoxanthin; Viola: violaxanthin; Allo: alloxanthin; Lut: lutein; Zea: zeaxanthin; Chl *b*: chlorophyll *b*; Chl *a*: chlorophyll *a*.

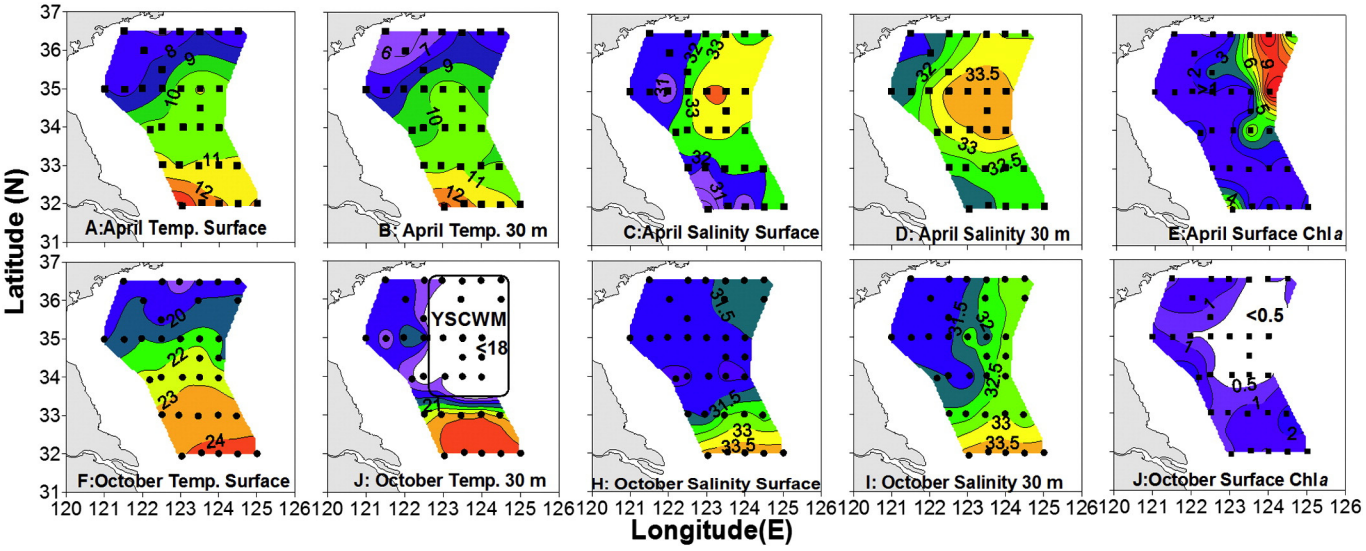

Fig. 2. Horizontal distribution (surface and 30 m) of temperature (°C), salinity, and the surface Chl *a* concentration (mg m^{-3}) in the southern Yellow Sea during the April and October cruises in 2006.

Due to the strong vertical mixing induced by the strong East Asian winter monsoon, a quite uniform distribution of temperature and salinity between the surface and 30 m was present during the April cruise (Fig. 2). Coincidentally, the water column showed a well-mixed vertical distribution through the 35°N transect during the March and April cruises (Fig. 3). More importantly, during the April cruise, warm (temperature >10 °C) and saline water (salinity >34) was observed at the bottom in the central area of the YS (Figs. 2 and 3). During the March cruise, this high temperature and salinity was again observed, which was associated with the so-called YSWC. The YSWC is the most obvious during winter (January–March). Therefore it seemed that, compared with the April cruise, the warm current water was shown much more clearly during the March cruise. During the April cruise (spring season) the high temperature and salinity water in the central YS probably was the remaining stream of the YSWC when it was declining (Fig. 3).

During the warm season, owing to the seasonal solar heating and weakened vertical mixing, strong stratification was established (Figs. 2 and 3). The well-known YSCWM was observed under the thermocline (Figs. 2 and 3). It was approximately present north of 34°N and east of 122.5°E in the study area (Fig. 2J). The bottom temperature in the center of the YSCWM was below 10 °C, and the salinity was higher than 33.5 (Fig. 3). Although both were impacted by the YSCWM, a much shallower and thicker thermocline was observed during August, thus the mixed layer depth was shallower in August than in October (Fig. 3). In

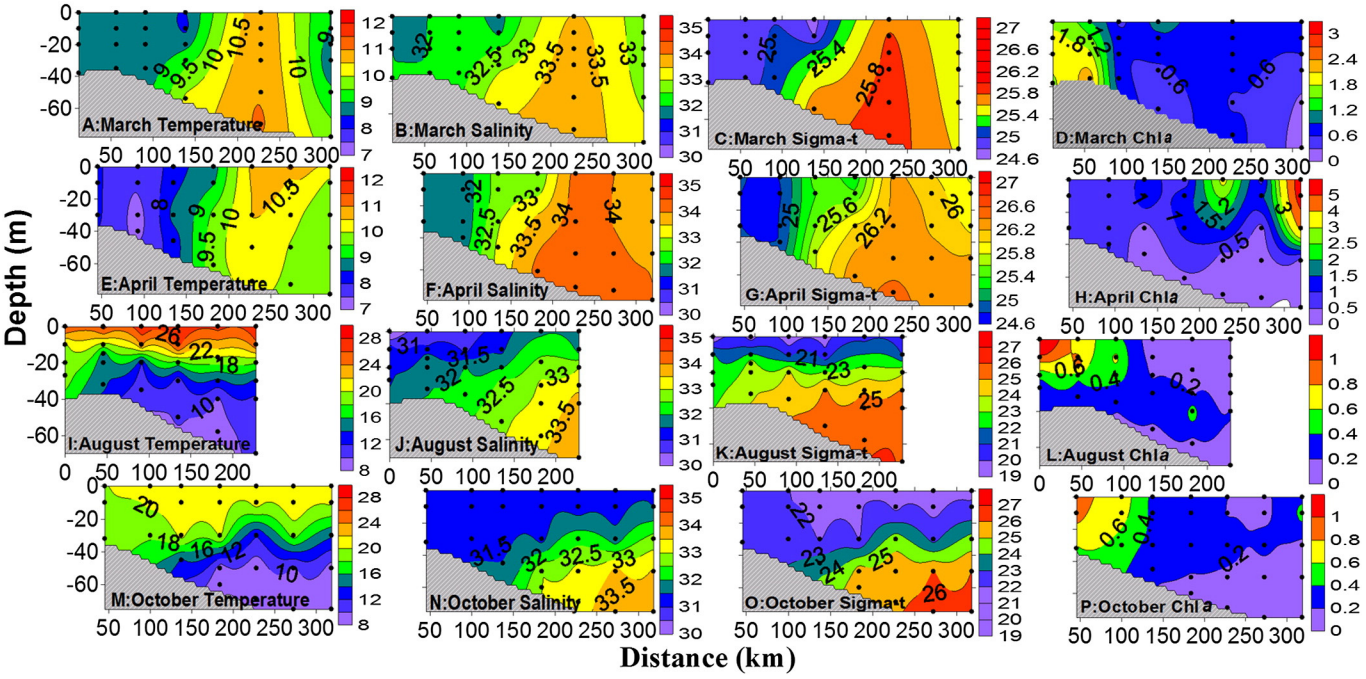

Fig. 3. Vertical distribution of temperature (°C), salinity, density (kg m^{-3}) and Chl *a* (mg m^{-3}) along the 35°N transect (D/Z transect, Fig. 1) in the southern Yellow Sea during the four cruises in 2006–2007.

Table 2
Depth, surface and bottom temperatures, and the means (in the euphotic zone) of nitrate, phosphate and silicic acid of stations in the coastal and central areas during the four cruises in April and October 2006, and March and August 2007.

Month	Area	Depth	Surface temperature	Bottom temperature	Nitrate (μmol L^{-1})	Phosphate (μmol L^{-1})	Silicic acid (μmol L^{-1})
		Mean ± SD	Mean ± SD	Mean ± SD	Mean ± SD	Mean ± SD	Mean ± SD
March 2007	Coastal (n = 9)	36.7 ± 8.0	8.84 ± 1.54	8.84 ± 1.74	5.1 ± 5.6	0.41 ± 0.23	6.7 ± 6.0
	Central (n = 7)	72.7 ± 9.9	10.05 ± 1.48	10.86 ± 1.11	5.1 ± 2.1[a]	0.50 ± 0.16[a]	9.0 ± 2.0[a]
April 2006	Coastal (n = 18)	37.3 ± 9.9	10.25 ± 2.17	9.68 ± 2.20	6.7 ± 1.9	0.25 ± 0.14	7.3 ± 5.5
	Central (n = 13)	72.9 ± 8.7	9.36 ± 1.56	9.19 ± 1.21	6.4 ± 1.3[a]	0.10 ± 0.04[b]	5.9 ± 3.3
August 2007	Coastal (n = 5)	35.6 ± 6.4	26.58 ± 0.69	14.88 ± 4.62	1.3 ± 0.7	0.21 ± 0.08	4.9 ± 0.8
	Central (n = 7)	73.4 ± 11.2	26.99 ± 0.56	11.11 ± 0.39	1.0 ± 0.7	0.19 ± 0.12	5.9 ± 2.0
October 2006	Coastal (n = 18)	37.6 ± 10.1	22.42 ± 1.83	21.19 ± 3.36	4.1 ± 3.9	0.27 ± 0.16	6.2 ± 4.9
	Central (n = 15)	72.5 ± 8.0	20.79 ± 1.53	8.72 ± 0.59[b]	1.1 ± 0.8[b]	0.09 ± 0.04[b]	4.3 ± 1.4

[a] Indicates that nutrient concentrations in the central area were significantly higher than those during the other cruises in the same area ($p < 0.05$).
[b] Indicates a significant difference between the coastal and central areas during the same cruise ($p < 0.05$).

addition, low salinity surface water in the coastal area was also noted, which was attributed to a large amount of freshwater input during the warm season (Figs. 2 and 3).

3.2. Nutrients and Chl a

3.2.1. Nutrient dynamics

During the cold season, both the coastal and central areas showed high nutrient concentrations (average value for the euphotic zone) as a result of the well-mixed structure in the water column (Table 2). The concentrations of nitrate and phosphate during the March cruise reached 6 μmol L^{-1} and 0.6 μmol L^{-1}, respectively, whereas they were less than 1 μmol L^{-1} and 0.1 μmol L^{-1} during August in the central YS (Fig. 4). Additionally, the nutrient-rich water observed in March was consistent with the occurrence of the YSWC (Figs. 3 and 4). Based on the results of the 35°N transect, relative higher nutrient concentrations were present in the central area rather than the coastal area (Fig. 4). Nutrient distribution patterns in April were generally similar to that in March, apart from reduction in phosphate concentration within the euphotic zone during April (Fig. 4E). There was a significant difference between the phosphate concentrations in the central YS and the coastal area (Table 2).

The diapycnal nutrient flux was restrained by the development of stratification during summer, and thus quite low concentrations of surface nutrients were observed in the central area (Table 2 and Fig. 4). The concentrations of nitrate (1.1 ± 0.8 μmol L^{-1}, mean ± SD) and phosphate (0.09 ± 0.04 μmol L^{-1}, mean ± SD) in the euphotic zone (~30 m) of the YSCWM area (n = 15) during the October cruise were significantly lower than those in the coastal area ($p < 0.01$, n = 18) (Table 2).

3.2.2. Chl a

Two contrasting spatial patterns were observed for surface Chl *a* concentrations during the April and October cruises in 2006 (Fig. 2). A clear spring phytoplankton bloom was observed during the April cruise in the northeast area (Fig. 2E). During this cruise, the surface Chl *a* ranged from 0.89 mg m^{-3} (at the southern stations) to 12.62 mg m^{-3} (at Station A5), with a mean of 2.97 ± 2.96 mg m^{-3} (n = 31). In

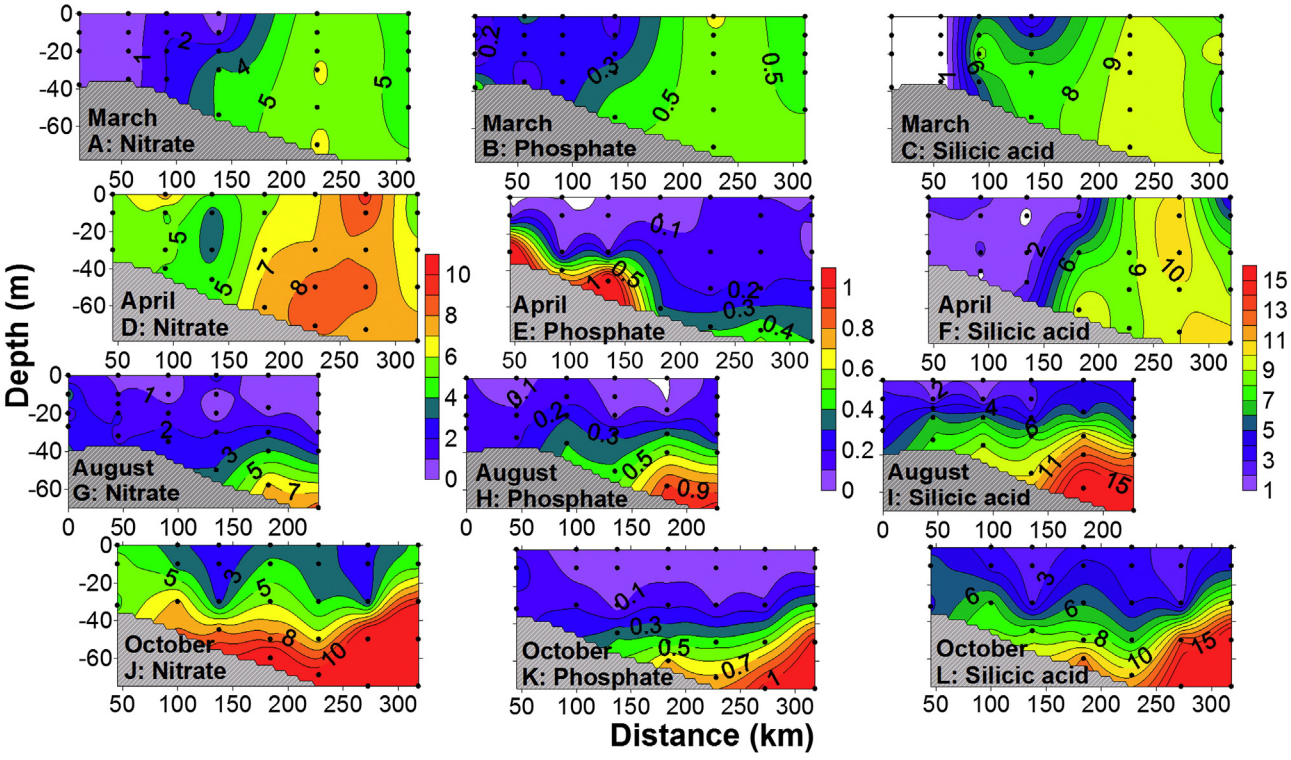

Fig. 4. Vertical distribution of nitrate, phosphate and silicic acid concentrations (μmol L^{-1}) along the 35°N transect (D/Z transect, Fig. 1) in the southern Yellow Sea during the four cruises in 2006–2007.

contrast, at most of the stations in the central YS during October, the Chl *a* concentrations were below 0.5 mg m^{-3} (Fig. 2J). The low Chl *a* area matched well with the area of deep low temperature water (Fig. 2).

Compared to the coastal area, the central YS showed more significant seasonal variation of Chl *a* (Fig. 5A). Both the highest (1.58 ± 1.09 mg m^{-3}, n = 13) and lowest Chl *a* (0.18 ± 0.05 mg m^{-3}, n = 7) were observed in this area during the April and August cruises, due to the spring bloom and the strong summer stratification, respectively. The seasonal patterns of sea surface Chl *a* measured by satellites at the coastal (D1) and central (D5) stations were consistent with the in situ measurements (Fig. 5). The Chl *a* was higher in the central than in the coastal station during April, with a large standard deviation, indicating the dynamic spring phytoplankton bloom. The climatological monthly mean SST and SSW speed showed typical features, which were related to the predictable seasonal changes of irradiance and the East Asian monsoon in the marginal seas of the northwestern Pacific Ocean (Fig. 5C). However, the SST was about 2 °C higher in February and March in the central area, where the impact of the YSWC was considered to be more significant.

3.3. Phytoplankton community structure

Not surprisingly, diatoms were the dominant group in the study area during the four cruises, with the average concentrations in the euphotic zone one magnitude higher than in the other groups (Fig. 6). The concentrations of diatoms were similar to those of the Chl *a* biomass with higher concentrations being observed in the coastal area during the March, August and October cruises, but in the central area during the April cruise (Figs. 2, 3 and 6).

During the April cruise in 2006, diatoms contributed 98% of the Chl *a* to the water column, with very high concentrations of Chl *a* (7.69 mg m^{-3}) and fucoxanthin (1.98 mg m^{-3}) at a spring bloom station (Stn. A5) in the northeast part of the study area (Fig. 6E). The diatom-dominated spring bloom was confirmed by microscopy and the chain-forming diatom, *Thalassiosira pacifica*, dominated the community. The abundance of this species was 1.3×10^6 cells L^{-1} and it made up 98.9% of the total phytoplankton abundance at Station A5, followed by *Guinardia delicatula* (6.39×10^3 cells L^{-1}) and *Corethron pennatum* (5.51×10^3 cells L^{-1}). The average concentration and relative abundance of diatoms in the central area during the spring bloom were as high as 2.13 mg m^{-3} and 76% (Fig. 7). In addition, the ratio of fucoxanthin to Chl *a* during April was significantly higher than the others (Fig. 8B), which was consistent with the results of CHEMTAX analysis (Fig. 7B).

During the March cruise, *Paralia sulcata* and *Coscinodiscus* spp. were the dominant species in the samples. The high contribution of diatoms (80%) coincided with the high Chl *a* in the coastal water (Fig. 6A), whereas the contribution of prasinophytes seemed to increase in the central area with a relatively lower Chl *a* concentration (Fig. 6D). The prasinophytes were the second most important group in the central area during March (Fig. 7B). The relative abundance (28 ± 7%) was significantly higher than those in April and August ($p < 0.01$).

During the warm seasons, quite low diatom concentrations occurred in the YSCWM area (Fig. 6). During the August cruise, the average concentration and relative abundance of diatoms in the central area were only 0.05 mg m^{-3} and 30%, when the YSCWM prevailed (Fig. 7). However, significantly higher concentrations of cyanobacteria were observed in August and south of the study area during the October cruise, associated with the higher temperature (Fig. 6). Therefore, the dominance of diatoms was replaced by that of cyanobacteria (36 ± 16%, n = 7) in the central area (Fig. 7B). During October, when the YSCWM was decaying, the concentrations of chrysophytes and prasinophytes increased (Fig. 6), and they contributed 38 and 18% of the Chl *a* biomass in the water column of the central YS (Fig. 7B). In addition, the ratios of 19′-hexanoyloxfucoxanthin and zeaxanthin to Chl *a*

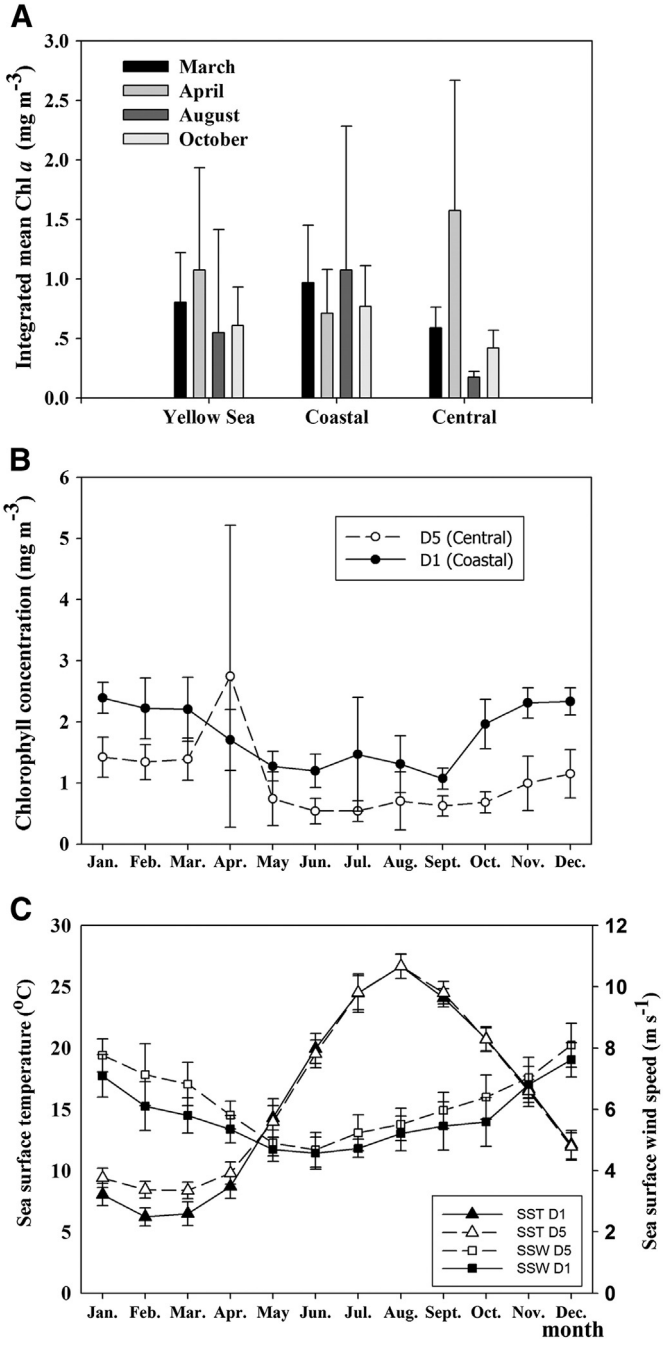

Fig. 5. Chl *a* concentrations (average value for the euphotic zone, mg m^{-3}) in the different subareas of the southern Yellow Sea during the four cruises in 2006–2007 (A) and climatological monthly mean Chl *a* (B), sea surface temperature (C, SST), sea surface wind (C, SSW) speed in Stations D1 (coastal) and D5 (central). Error bars on the Chl *a* concentrations are standard deviation.

during the warm seasons were relatively higher than those in the cold seasons (Fig. 8B).

4. Discussion

As we hypothesized, significant seasonal variations on phytoplankton biomass (Fig. 5) and community structure (Figs. 6–8) were observed in the central area compared to the coastal area. Indeed, the YSWC and YSCWM seemed to be important players in determining the spatial and temporal patterns of phytoplankton biomass and community structure in the central YS.

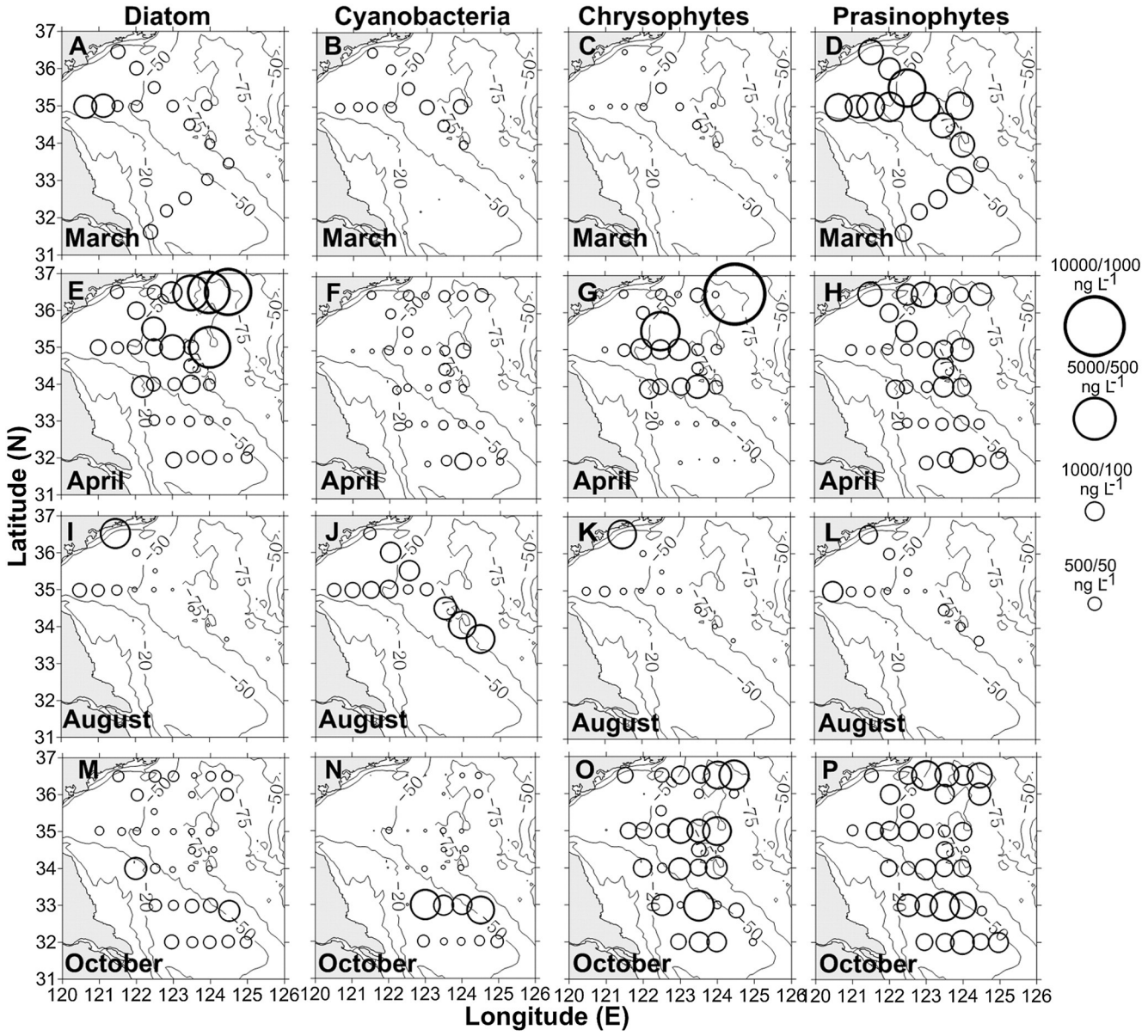

Fig. 6. The spatial distribution of Chl *a* concentrations (average value for the euphotic zone, mg m^{-3}) of the four major phytoplankton groups (diatoms, cyanobacteria, chrysophytes and prasinophytes) during the four cruises in 2006–2007. The scale of diatom concentrations is one magnitude greater than that of the others.

4.1. Yellow Sea Warm Current and spring phytoplankton bloom

In previous studies, high nutrient concentrations were also observed in the central YS in winter and spring (Fu et al., 2009; Hyun and Kim, 2003; Jin et al., 2013). They suggest that this high nutrient water might have originated from the bottom mixed water in the winter season. The nutrient-rich bottom water is a result of nutrient accumulation in the YSCWM during the previous summer and fall. However, in the present study the nutrient-rich water was observed coincidently with the occurrence of the YSWC (Figs. 3 and 6), which is confirmed to be linked to the water intrusion of the Cheju Warm Current, a Kuroshio branch current (Lie et al., 2009). A recent study revealed that the mean depth integrated concentrations of DIN, PO_4^{3-} and SiO_3^{2-} in the YSWC area were 660, 40 and 840 mmol m^{-2}, respectively, which were 1.5 times as high as that in the non-YSWC area (Jin et al., 2013). Undoubtedly, the strong wind-driven vertical mixing can provide a lot of nutrients (Jin et al., 2013), however, in complex marginal sea ecosystems, not only the vertical nutrient fluxes, but also the horizontal direction is very important. Physical researchers note that the Kuroshio moves onshore both in the nutrient-poor surface layer and in the nutrient-rich subsurface layer (Lee and Matsuno, 2007) and there are abundant nutrients during winter south of the main axis of the YSWC (Changjiang River estuary) (Chen, 2009; Wang et al., 2003). Therefore, there is another possible explanation in that the warm and nutrient-rich water might partially originate from the subsurface nutrient-rich water of the Kuroshio and/or from the Changjiang (Yangtze) River estuary. Future work aims to gather evidence about the sources of the high nutrient waters.

Although nutrient concentrations were high, Chl *a* concentration was low (Fig. 3D, <0.6 mg m^{-3}) in the YSWC area. During the March cruise a vertically homogenous water column was observed, and therefore phytoplankton might not have accumulated in the euphotic zone because the mixed-layer depth was deeper than the critical depth (Figs. 3, 4 and 9) (Fu et al., 2009; Hyun and Kim, 2003; Sverdrup, 1953). On the other hand, the turbid coastal water induced by strong mixing does not favor phytoplankton growth because of the instability

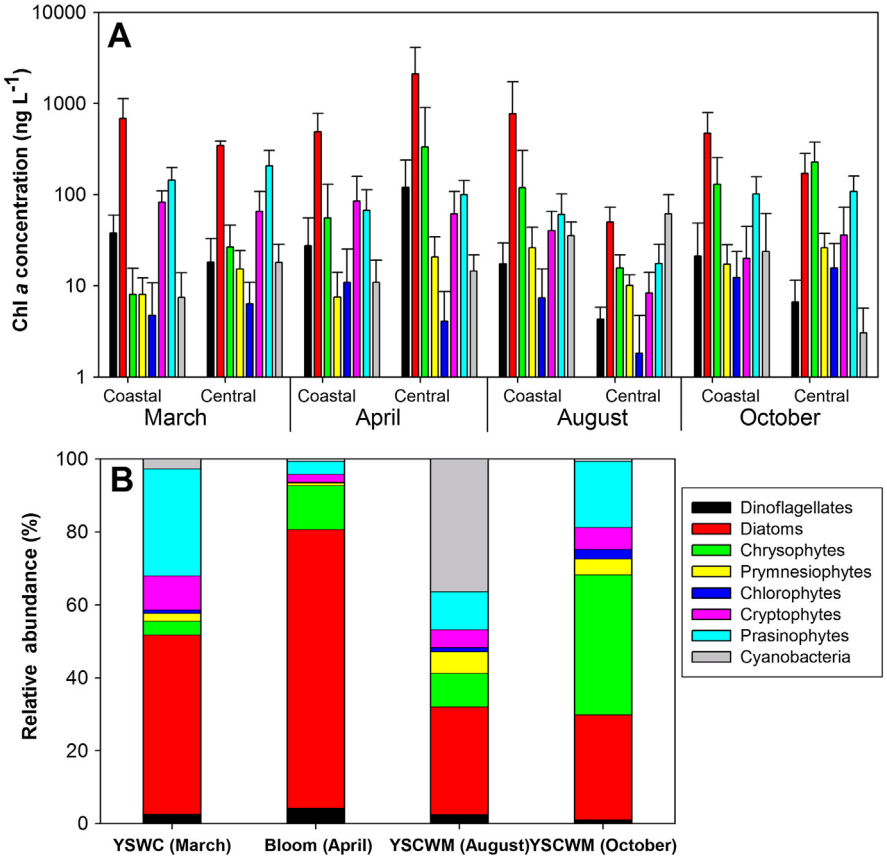

Fig. 7. Seasonal variation of integrated mean Chl *a* of various algal classes in the different subareas (A, average value for the euphotic zone, mg m^{-3}) and the contribution of various algal classes to total Chl *a* biomass in the central area (B, relative abundance, %) during the four cruises in 2006–2007. The vertical axis for Chl *a* concentration is presented as a logarithmic scale.

and light limitation in the water column. In addition, our results showed that the phytoplankton community was dominated by *P. sulcata* and *Coscinodiscus* spp. during the March cruise. *P. sulcata* is a typical benthic type which is induced by strong mixing of bottom and preponderant in unstable hydrologic conditions (Tang et al., 2013).

It should be noted that the prasinophytes were abundant in the central area associated with the occurrence of the YSWC (Fig. 7). Based on pigment data, the highest (172 ± 81 ng L^{-1}, n = 16) and lowest (35 ± 34 ng L^{-1}, n = 33) prasinophyte Chl *a* concentrations were found during the March and August cruises, while they contributed about 30 and 6% of the total Chl *a* biomass. The Chl *b* to Chl *a* ratio in the central area was significantly higher during the March cruise than during the other cruises (Fig. 8B), and the Chl *b* concentration was observed to be the second most important pigment in most of the samples, indicating that the prasinophytes and/or chlorophytes might contribute a high percentage in the YS. However, quite low lutein concentrations were detected (<3 ng L^{-1}), which was almost one magnitude lower than that of prasinoxanthin (~10–20 ng L^{-1}). Using HPLC-CHEMTAX analysis, the prasinophytes were significantly higher in abundance than the chlorophytes ($p < 0.01$, n = 16). The prasinophytes are known to be common in temperate and cold regions where they can occur as prominent constituents of the marine picoplankton (Throndsen, 1976). One well known genus of prasinophytes is *Ostreococcus*, considered to be the smallest (ca. 0.95 μm) free-living eukaryote, found in marine waters worldwide (Courties et al., 1994). Two clades of *Ostreococcus* were thought to be distinguished in the environment by their adaptation to light intensities, with the high-light ecotypes being detected at warm oligotrophic sites whereas the low-light ecotypes were present in cooler mesotrophic and coastal waters (Rodriguez et al., 2005). The YSWC originated from the Kuroshio but rich in nutrients, thus it is difficult to speculate which clade dominated or coexist. In the future, using fluorescence in situ hybridization with primer-probes (Demir-Hilton et al., 2011) may find out the difference in distributions of these two clades in the central YS.

During early spring, the combination of rising irradiance and temperature and weak stratification increases the residence time of the phytoplankton and its growth rate within the euphotic layer, and seems to trigger the spring phytoplankton bloom in the central YS (Fig. 9; Hyun and Kim, 2003; Xuan et al., 2011; Tang et al., 2013). Based on in situ and satellite observations, the spring phytoplankton bloom during 2007 and 2009 occurred at the tip of YSWC, where the warm and nutrient-rich water met the cold and turbid coastal water (Xuan et al., 2011, 2012). This kind of front is usually characterized by high levels of biological activity and active exchange of energy and matter (Franks, 1992). Using a 3-dimensional physical–biological coupled model, Hu et al. (2004) reveal that the initiation of the spring phytoplankton bloom is critically related to the water column stability. The weak stratification caused by the decrease of the wind speed and interaction between water masses is more suitable than the well mixed structure for phytoplankton growth (Hyun and Kim, 2003; Sverdrup, 1953). Xuan et al. (2011, 2012) also point out that Sverdrup's critical depth model can be applied to explain phytoplankton growth in the central YS using the 3-D physical ocean model MITgcm.

In previous studies, the impacts of YSWC on the spring bloom were mainly related to the hydrodynamic environment rather than the nutrients. Recently, nutrient status during the spring bloom in the central YS has been reported (Jin et al., 2013). Their results show that nutrient concentrations before the spring bloom within the euphotic zone of the YSWC area are significantly higher than those in the coastal area, and rapidly decreasing during the blooms (Jin et al., 2013). Similarly, the decline of nutrients in the central area during April, compared with

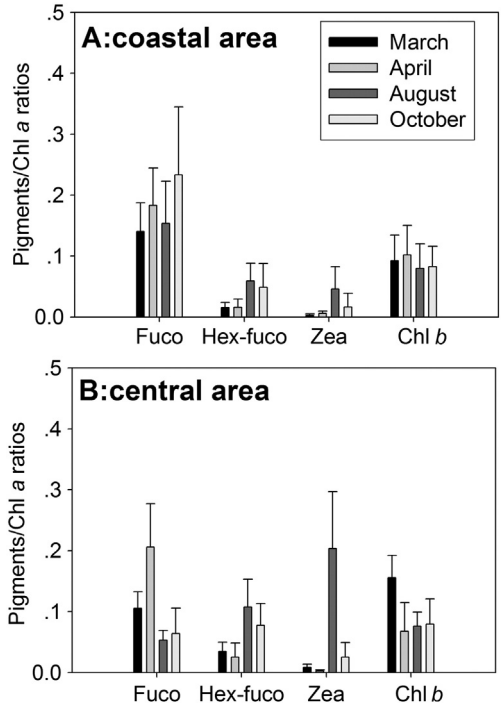

Fig. 8. The seasonal variation of major pigments to Chl *a* ratios in the coastal (A) and central (B) areas during the four cruises in 2006–2007. Pigment abbreviations are indicated in Table 1.

that during March (Table 2), might be caused by phytoplankton uptake. However, the detailed process during the spring bloom still looks very complex and dynamic (Jin et al., 2013). The spring bloom lasts for about two months from April to May each year and is composed of a series of sub-bloom events that show different dominant species compositions, likely corresponding to the different stages of spring blooms (Tang et al., 2013). Our results show that phosphate was exhausted first and extremely lacking in the euphotic zone of central YS during April, while there was a surplus of nitrate and silicate (Fig. 4E). The possible explanation might be attributed to the nitrogen deposition (Fanning, 1989). Ren et al. (2011) report that a large-scale diatom bloom occurred four to five days after an Asian dust event during spring 2007, indicating the deposition supply of nutrients for phytoplankton growth (Zhang, 1994). More importantly, the increase in N availability caused by atmospheric deposition has switched extensive parts of this study area from being N-limited to P-limited (Kim et al., 2011). It is likely, therefore, that the mechanism and processes of the spring bloom are very complex and possibly unique in the central YS (Fig. 9). Nevertheless, coupled with the effects of nutrients and hydrological environment, the YSWC is suggested to be one of the players in the YS spring phytoplankton bloom. To improve our basic understanding of the spring bloom in the complex marginal sea, it is important to clarify the sources of nutrients and evaluate phytoplankton consumption at the same time.

4.2. Yellow Sea Cold Water Mass

The seasonal evolution of the YSCWM can be attributed to the unique basin topography and the impact of both the seasonal evolution of thermocline and the circulation system in the YS (Zhang et al., 2008). Basically, the seasonal thermocline is an important physical barrier in the ocean, separating the well-lit, nutrient-poor and warm surface layer from the darker, nutrient-rich and cold deeper water. The stable and high density gradient inhibits the diapycnal transfer of nutrients (Liu et al., 2003, 2012; Wang et al., 2003). Besides the low nutrient concentrations, previous studies show high proportions of dissolved organic nitrogen and dissolved organic phosphorus (Liu et al., 2003) and the DIN/PO_4^{3-} ratio above the subsurface chlorophyll maximum is almost three times higher than that of the bottom layer (Liu et al., 2012), implying an extreme shortage of phosphate. Consequently, in the surface mixed layer of the central YS, it is easy to suggest that the growth of phytoplankton was limited by the poor nutrient concentrations, and so the smaller phytoplankters (e.g. the cyanobacteria) became dominant. Although the cyanobacteria dominated ($64 \pm 3\%$, $n = 10$) the upper layer of the southern YS (Fig. 6H), diatoms and chrysophytes contributed $38 \pm 6\%$ and $21 \pm 4\%$ ($n = 5$) of the Chl *a* concentration at the subsurface chlorophyll maximum ($0.52 \pm 0.4\ \mu g\ L^{-1}$, $n = 5$) at Station D5 (Liu et al., 2012). When the YSCWM was decaying, a much lower surface temperature and a deeper thermocline were observed (Fig. 3), and nutrient concentrations within the surface mixed layer in October were not as low as in August. This might be the explanation for the differences in phytoplankton community composition between August and October (Figs. 6 and 7).

In terms of spatial distribution, the phytoplankton pigment ratios and community composition (which was strongly influenced by environmental conditions) showed patterns similar to the T–S properties (Figs. 6 and 7). In coastal areas of the YS the concentrations of N, P and Si compounds are high, reflecting the effects of the Changjiang effluent plume, surface runoff from the west and east coasts, and circulation in the YS (Liu et al., 2003). However, because of the unique basin topography and strong tidal currents, the YSCWM is fringed by typical tidal mixing fronts, which separate the cold, stratified water at the offshore side from the warm, well-mixed, shallow water on the other side (Qiao et al., 2006). Thus, significantly lower nutrient and Chl *a* concentrations are observed on the surface of the YSCWM area than in the surrounding water in summer (Fu et al., 2009). In the present study, much evidence was presented of the YSCWM area behaving differently from the rest of the sampled region, especially with regard to phytoplankton community structure (Figs. 2–8).

In addition, if the pico-size phytoplanktons dominate, then the importance of microbial loop may become more prominent. Bacteria, flagellates, ciliates and pico-plankton may have a more significant impact on higher trophic levels. Multivariate analysis based on the copepod assemblage resulted in the recognition of five groups corresponding to the different water masses in the East China Sea and YS, and the one in the YSCWM is the most notable one (Zuo et al., 2006). During summer, the low Chl *a* biomass in the central YS leads to the copepodite stage V (C5) dominating the population, and the reproduction of the dominant species (*Calanus sinicus*) nearly ceases during summer, with most of the females remaining at stages GS1 and GS2 inside

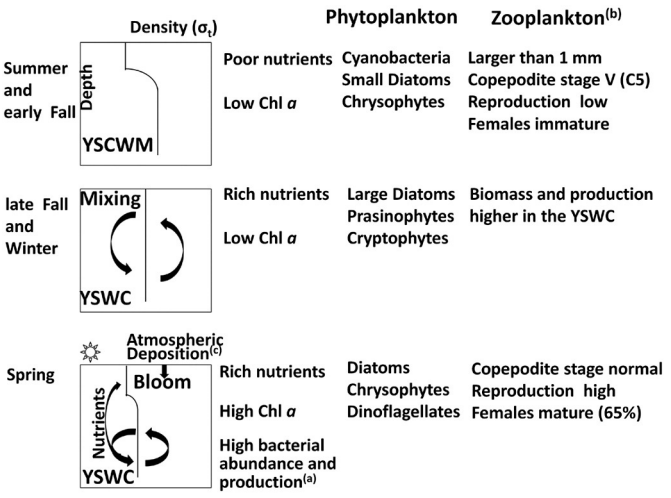

Fig. 9. Seasonal circulation patterns of the major physical processes and their biogeochemical responses in the central Yellow Sea. YSCWM: Yellow Sea Cold Water Mass, YSWC: Yellow Sea Warm Current. (a) Hyun and Kim (2003), (b) Wang et al. (2009); Huo et al. (2012), (c) Zhang (1994); Ren et al. (2011).

the YSCWM (Fig. 9; Wang et al., 2009; Huo et al., 2012). Further, Jin et al. (2003) reveal that the fish composition and diversity are different between the central YS and the other areas during fall, indicating that the YSCWM ecosystem may also play an important role in the distribution of fish species in the YS.

In conclusion, a very strong spatial heterogeneity was observed among the physical, chemical and biological parameters in the study area when the YSCWM occurred. In the central part, typically the abundance and/or community structure of organisms (phyto-/zoo-plankton) were derived from the supply of resources (e.g. nutrients) and/or by physical factors (e.g. temperature and/or salinity) during the YSCWM season, which are the fundamental characteristics of a bottom–up control system (Fig. 9). At this point, the system in the central YS in summer was similar to the open ocean when the YSCWM prevailed. All this evidence suggested that the ecosystem of the central area was different from the other regions in the southern YS (Fig. 9).

5. Conclusions

Significant seasonal biological responses to physical processes were observed in the central YS (Fig. 9). During winter, nutrient-rich water was observed coincidently with the occurrence of the YSWC (Fig. 4). Prasinophytes were abundant and the main contributors of Chl *b* in the YSWC water. The mechanism/process of the spring bloom was very complex and unique. However, the YSWC was suggested to be one of the important players. A very strong spatial heterogeneity was observed in the physical, chemical and biological parameters in the central YS during the YSCWM occurrence (Figs. 2, 7 and Table 2). A low Chl *a* biomass (0.2 mg m^{-3}) and a low contribution of diatoms to the total Chl *a* biomass (30%), with a high contribution of cyanobacteria (36%), were observed in the central YS in August when the YSCWM prevailed, and a high contribution of chrysophytes (38%) was observed in October when it was decaying. All these results were considered as the characteristic physical–chemical–biological response of the ecosystem in the central YS.

Acknowledgments

The authors would like to thank the captain and crew of the RV "Beidou", who made concerted efforts to assist during field sampling. We are grateful to Professor Kuo-Ping Chiang of the National Taiwan Ocean University and Ken Furuya of the University of Tokyo for their helpful discussion and critical comments on the manuscript, and Professor John Hodgkiss of The University of Hong Kong for his language editing and comments on the manuscript. We also show our thanks to the anonymous reviewers. This work was supported by grants from the National Basic Research Programme (China GLOBEC-IMERS Program, Nos. 2011CB403603 and 2006CB400604), the China NSF (Nos. 40925018 and 41406143) and China Postdoctoral Science Foundation funded project (2014M551839).

References

Chen, C.T.A., 2009. Chemical and physical fronts in the Bohai, Yellow and East China seas. J. Mar. Syst. 78, 394–410.
Courties, C., Vaquer, A., Troussellier, M., Lautier, J., Chrétiennot-Dinet, M.J., Neveux, J., Machado, C., Claustre, H., 1994. Smallest eukaryotic organism. Nature 370 (6487), 255.
Demir-Hilton, E., Sudek, S., Cuvelier, M.L., Gentemann, C.L., Zehr, J.P., Worden, A.Z., 2011. Global distribution patterns of distinct clades of the photosynthetic picoeukaryote *Ostreococcus*. ISME J. 5 (7), 1095–1107.
Fanning, K.A., 1989. Influence of atmospheric pollution on nutrient limitation in the ocean. Nature 339, 460–463.
Franks, P.J.S., 1992. Phytoplankton blooms at fronts — patterns, scales, and physical forcing mechanisms. Rev. Aquat. Sci. 6, 121–137.
Fu, M.Z., Wang, Z.L., Li, Y., Li, R.X., Sun, P., Wei, X.H., Lin, X.Z., Guo, J.S., 2009. Phytoplankton biomass size structure and its regulation in the Southern Yellow Sea (China): seasonal variability. Cont. Shelf Res. 29, 2178–2194.
Furuya, K., Hayashi, M., Yabushita, Y., Ishikawa, A., 2003. Phytoplankton dynamics in the East China Sea in spring and summer as revealed by HPLC-derived pigment signatures. Deep-Sea Res. II 50, 367–387.
He, X.Q., Bai, Y., Pan, D.L., Chen, C.T.A., Chen, Q., Wang, D.F., Gong, F., 2013. Satellite views of seasonal and inter-annual variability of phytoplankton blooms in the eastern China seas over the past 14 yr (1998–2011). Biogeosci. Discuss. 10, 111–155.
Hu, H.G., Wan, Z.W., Yuan, Y.L., 2004. Simulation of seasonal variation of phytoplankton in the southern Huanghai (Yellow) Sea and analysis on its influential factors. Acta Oceanol. Sin. 26, 74–88.
Huang, D.J., Fan, X.P., Xu, D.F., Tong, Y.Z., Su, J.L., 2005. Westward shift of the Yellow Sea warm salty tongue. Geophys. Res. Lett. 32 (24). http://dx.doi.org/10.1029/2005gl024749.
Huang, B.Q., Hu, J., Xu, H.Z., Cao, Z.R., Wang, D.X., 2010. Phytoplankton community at warm eddies in the northern South China Sea in winter 2003/2004. Deep-Sea Res. II 57 (19–20), 1792–1798.
Huo, Y., Sun, S., Zhang, F., Wang, M., Li, C., Yang, B., 2012. Biomass and estimated production properties of size-fractionated zooplankton in the Yellow Sea, China. J. Mar. Syst. 94, 1–8.
Hyun, J.H., Kim, K.H., 2003. Bacterial abundance and production during the unique spring phytoplankton bloom in the central Yellow Sea. Mar. Ecol. Prog. Ser. 252, 77–88.
Jin, X., Xu, B., Tang, Q., 2003. Fish assemblage structure in the East China Sea and southern Yellow Sea during autumn and spring. J. Fish Biol. 62, 1194–1205.
Jin, J., Liu, S.M., Ren, J.L., Liu, C.G., Zhang, J., Zhang, G.L., Huang, D.J., 2013. Nutrient dynamics and coupling with phytoplankton species composition during the spring blooms in the Yellow Sea. Deep-Sea Res. II 97, 16–32.
Kim, T.W., Lee, K., Najjar, R.G., Jeong, H.D., Jeong, H.J., 2011. Increasing N abundance in the northwestern Pacific Ocean due to atmospheric nitrogen deposition. Science 334 (6055), 505–509.
Latasa, M., 2007. Improving estimations of phytoplankton class abundances using CHEMTAX. Mar. Ecol. Prog. Ser. 329, 13–21.
Lee, J.S., Matsuno, T., 2007. Intrusion of Kuroshio water onto the continental shelf of the East China Sea. J. Oceanogr. 63, 309–325.
Lie, H.J., 1986. Summertime hydrographic features in the southeastern Hwanghae. Prog. Oceanogr. 17, 229–242.
Lie, H.J., Cho, C.H., Lee, S., 2009. Tongue-shaped frontal structure and warm water intrusion in the southern Yellow Sea in winter. J. Geophys. Res. 114, C01003. http://dx.doi.org/10.1029/2007JC004683.
Lin, C., Ning, X., Su, J., Lin, Y., Xu, B., 2005. Environmental changes and the responses of the ecosystems of the Yellow Sea during 1976–2000. J. Mar. Syst. 55, 223–234.
Liu, S.M., Zhang, J., Chen, S.Z., Chen, H.T., Hong, G.H., Wei, H., Wu, Q.M., 2003. Inventory of nutrient compounds in the Yellow Sea. Cont. Shelf Res. 23, 1161–1174.
Liu, S.M., Zhang, J., Chen, H.T., Zhang, G.S., 2005. Factors influencing nutrient dynamics in the eutrophic Jiaozhou Bay, North China. Prog. Oceanogr. 66, 66–85.
Liu, Z.Y., Wei, H., Lozovatsky, I.D., Fernando, H.J.S., 2009. Late summer stratification, internal waves, and turbulence in the Yellow Sea. J. Mar. Syst. 77, 459–472.
Liu, X., Huang, B.Q., Liu, Z., Wang, L.Y., Wei, H., Li, C.L., Huang, Q., 2012. High-resolution phytoplankton diel variations in the summer stratified central Yellow Sea. J. Oceanogr. 68, 913–927.
Mackey, M.D., Mackey, D.J., Higgins, H.W., Wright, S.W., 1996. CHEMTAX — a program for estimating class abundances from chemical markers: application to HPLC measurements of phytoplankton. Mar. Ecol. Prog. Ser. 144, 265–283.
Mantoura, R.E.C., Llewellyn, C.A., 1983. The rapid determination of algal chlorophyll and carotenoid pigments and their breakdown products in natural waters by reverse-phase high-performance liquid chromatography. Anal. Chim. Acta. 151, 297–314.
Ocean Watch North Pacific Demonstration Project, 2008. Ocean Watch North Pacific Demonstration Project products available from Ocean Watch web site. http://las.pfeg.noaa.gov/oceanwatch/oceanwatch.php.
Park, Y.H., 1986. Water characteristics and movements of the Yellow Sea Warm Current in summer. Prog. Oceanogr. 17, 243–254.
Qiao, F.L., Ma, J., Xia, C.S., Yang, Y.Z., Yuan, Y.L., 2006. Influence of the surface wave induced and tidal mixing on vertical temperature structure of the Yellow and East China Seas in summer. Prog. Nat. Sci. 16 (7), 739–746.
Ren, J.L., Zhang, G.L., Zhang, J., Shi, J.H., Liu, S.M., Li, F.M., Jin, J., Liu, C.G., 2011. Distribution of dissolved aluminum in the Southern Yellow Sea: influences of a dust storm and the spring bloom. Mar. Chem. 125, 69–81.
Rodriguez, F., Derelle, E., Guillou, L., Le Gall, F., Vaulot, D., Moreau, H., 2005. Ecotype diversity in the marine picoeukaryote *Ostreococcus* (Chlorophyta, Prasinophyceae). Environ. Microbiol. 7, 853–859.
Sun, X.X., Wang, S.W., Sun, S., 2011. The key processes, mechanism and ecological consequences of jellyfish bloom in China coastal waters. Chin. J. Oceanol. Limnol. 29, 491–492.
Sverdrup, H.U., 1953. On conditions for the vernal blooming of phytoplankton. ICES J. Mar. Sci. 18, 287–295.
Tang, Q.S., Su, J.L., Kishi, M.J., Oh, I.S., 2007. An introduction to the Second China–Japan–Korea Joint GLOBEC Symposium on the ecosystem structure, food web trophodynamics and physical-biological processes in the Northwest Pacific. J. Mar. Syst. 67, 203–204.
Tang, Q.S., Su, J.L., Zhang, J., 2010. China GLOBEC II: a case study of the Yellow Sea and East China Sea ecosystem dynamics preface. Deep-Sea Res. II 57, 993–995.
Tang, Q.S., Su, J.L., Zhang, J., 2013. Spring blooms and the ecosystem processes: the case study of the Yellow Sea. Deep-Sea Res. II 97, 1–3.
Throndsen, J., 1976. Occurrence and productivity of small marine flagellates. Nor. J. Bot. 23, 269–293.
Uda, M., 1934. The results of simultaneous oceanographical investigations in the Japan Sea and its adjacent waters in May and June 1932 (in Japanese). J. Imp. Fisher. Exp. Stn. 5, 138–190.

Utermöhl, H., 1958. Zur vervollkommnung der quantitativen phytoplankton—methodik. Mitt. Internationale Ver. Theoretische und Angewandte Limnologie 9, 1–38.
Van Heukelem, L., Thomas, C.S., 2001. Computer-assisted high-performance liquid chromatography method development with applications to the isolation and analysis of phytoplankton pigments. J. Chromatogr. A 910, 31–49.
Wang, B.D., Wang, X.L., Zhan, R., 2003. Nutrient conditions in the Yellow Sea and the East China Sea. Estuar. Coast. Shelf Sci. 58 (1), 127–136.
Wang, S.W., Li, C.L., Sun, S., Ning, X.R., Zhang, W.C., 2009. Spring and autumn reproduction of *Calanus sinicus* in the Yellow Sea. Mar. Ecol. Prog. Ser. 379, 123–133.
Xuan, J.L., Zhou, F., Huang, D.J., Wei, H., Liu, C.G., Xing, C.X., 2011. Physical processes and their role on the spatial and temporal variability of the spring phytoplankton bloom in the central Yellow Sea. Acta Ecol. Sin. 31 (1), 61–70.
Xuan, J.L., Zhou, F., Huang, D., Zhu, X.H., Xing, C., Fan, X., 2012. Modelling the timing of major spring bloom events in the central Yellow Sea. Estuar. Coast. Shelf Sci. 113, 283–292.
Zapata, M., Rodriguez, F., Garrido, J.L., 2000. Separation of chlorophylls and carotenoids from marine phytoplankton: a new HPLC method using a reversed phase C-8 column and pyridine-containing mobile phase. Mar. Ecol. Prog. Ser. 195, 29–45.
Zhang, J., 1994. Atmospheric wet deposition of nutrient elements — correlation with harmful biological blooms in Northwest Pacific coastal zones. Ambio 23, 464–468.
Zhang, S.W., Wang, Q.Y., Lu, Y., Cui, H., Yuan, Y.L., 2008. Observation of the seasonal evolution of the Yellow Sea Cold Water Mass in 1996–1998. Cont. Shelf Res. 28, 442–457.
Zhang, F., Li, C.L., Sun, S., Wu, Y.L., Ren, J.P., 2009. Distribution patterns of chlorophyll a in spring and autumn in association with hydrological features in the southern Yellow Sea and northern East China Sea. Chin. J. Oceanol. Limnol. 27, 784–792.
Zuo, T., Wang, R., Chen, Y.Q., Gao, S.W., Wang, K., 2006. Autumn net copepod abundance and assemblages in relation to water masses on the continental shelf of the Yellow Sea and East China Sea. J. Mar. Syst. 59, 159–172.